ORIGINAL ARTICLE

Improved anti-solid tumor response by humanized anti-podoplanin chimeric antigen receptor transduced human cytotoxic T cells in an animal model

Akihiro Ishikawa[1] | Masazumi Waseda[1] | Tomoko Ishii[1] |
Mika K. Kaneko[2] | Yukinari Kato[2,3] | Shin Kaneko[1]

[1]Shin Kaneko Laboratory, Department of Cell Growth and Differentiation, Center for iPS Cell Research and Application (CiRA), Kyoto University, Kyoto, Japan

[2]Department of Antibody Drug Development, Tohoku University Graduate School of Medicine, Sendai, Japan

[3]Department of Molecular Pharmacology, Tohoku University Graduate School of Medicine, Sendai, Japan

Correspondence
Shin Kaneko, Shin Kaneko Laboratory, Department of Cell Growth and Differentiation, Center for iPS Cell Research and Application (CiRA), Kyoto University, Kyoto, Japan.
Email: kaneko.shin@cira.kyoto-u.ac.jp

Abstract

Recently, research has been conducted with chimeric antigen receptor (CAR)-T cells to improve efficacy against solid tumors. Humanized CAR improved the long-term survival of CAR-T cells in patients' peripheral blood, resulting in increased therapeutic efficacy. Therefore, the humanization of the CAR-gene sequence is considered an effective method. Podoplanin (PDPN) is a glycosylated transmembrane protein that is highly expressed in solid tumors and is associated with poor prognosis in patients with cancer. Therefore, PDPN is considered a biomarker and good target for cancer treatment with CAR-T cells. Previously, an anti-PDPN CAR was generated from a conventional nonhumanized antibody—NZ-1, the only anti-PDPN antibody for which a CAR was produced. In this study, we investigated other anti-PDPN CARs from the antibody NZ-27, or humanized NZ-1, to enhance the therapeutic potential of CAR-T cells. The CAR signal intensity was enhanced by the efficient expression of CAR proteins on the T-cell surface of NZ-27 CAR-T cells, which show tumor-specific cytotoxicity, proinflammatory cytokine production, and anti-tumor activity against PDPN-expressing tumor xenografts in mice that were significantly better than those in nonhumanized NZ-1 CAR-T cells.

KEYWORDS
CAR-T cells, chimeric antigen receptor, humanized antibody, podoplanin, solid tumor

1 | INTRODUCTION

A chimeric antigen receptor (CAR) is an artificially generated receptor with a monoclonal antibody-derived single-chain variable fragment (scFv) in its extracellular domain and CD3z or co-stimulatory molecules in its intracellular domain (June et al., 2018; Scarfò & Maus, 2017). CAR-T

cells targeting CD19-positive B-cell malignancies were the first therapeutic CAR-T cell products with excellent therapeutic efficacy in prolonging patient survival. Recently, better therapeutic efficacy was reported to be achieved by the prolonged persistence of CAR-T cells in patients. One strategy to prolong CAR-T endurance involves the humanization of the animal-derived scFv sequences of CAR. Additionally, clinical trials have reported higher therapeutic efficacy using humanized CD19 CAR-T cells than original CD19 CAR-T cells (Myers et al., 2021).

Akihiro Ishikawa and Masazumi Waseda contributed equally to this work.

Podoplanin (PDPN) is a mucin-type transmembrane protein with a glycosylated extracellular domain that is over-expressed in various cancers, such as brain, oral, and lung cancers (Breiteneder-Geleff et al., 1997; Chu et al., 2005; Kahn et al., 2002; Kato et al., 2003, 2004; Mishima et al., 2006; Schacht et al., 2005), and is considered a promising therapeutic target for cancer treatment (Kreppel et al., 2010; Mori et al., 2021; Waseda & Kaneko, 2020). To target PDPN, we previously focused on the rat anti-human PDPN antibody (NZ-1), which recognizes PDPN specifically (Kato et al., 2006). The therapeutic efficacy of NZ-1-scFv-immunotoxin and NZ-1-derived CAR-T cells has been reported in PDPN xenograft tumor-engrafted mouse models (Chandramohan et al., 2013; Shiina et al., 2016).

The effectiveness of CAR-T cells partially depends on CAR expression on the T cell surface and CAR signal intensity (Jayaraman et al., 2020). In this study, to increase the therapeutic potential of anti-PDPN CAR-T cells, we generated a CAR from the NZ-27 antibody, which is a humanized NZ-1 antibody. This study clarified the improvement of CAR signal intensity by efficiently expressing CAR proteins on the T-cell surface and reported that the therapeutic efficacy of NZ-27 CAR-T cells was better than that of NZ-1 CAR-T cells against PDPN-expressing cells in vitro and in vivo.

2 | RESULTS

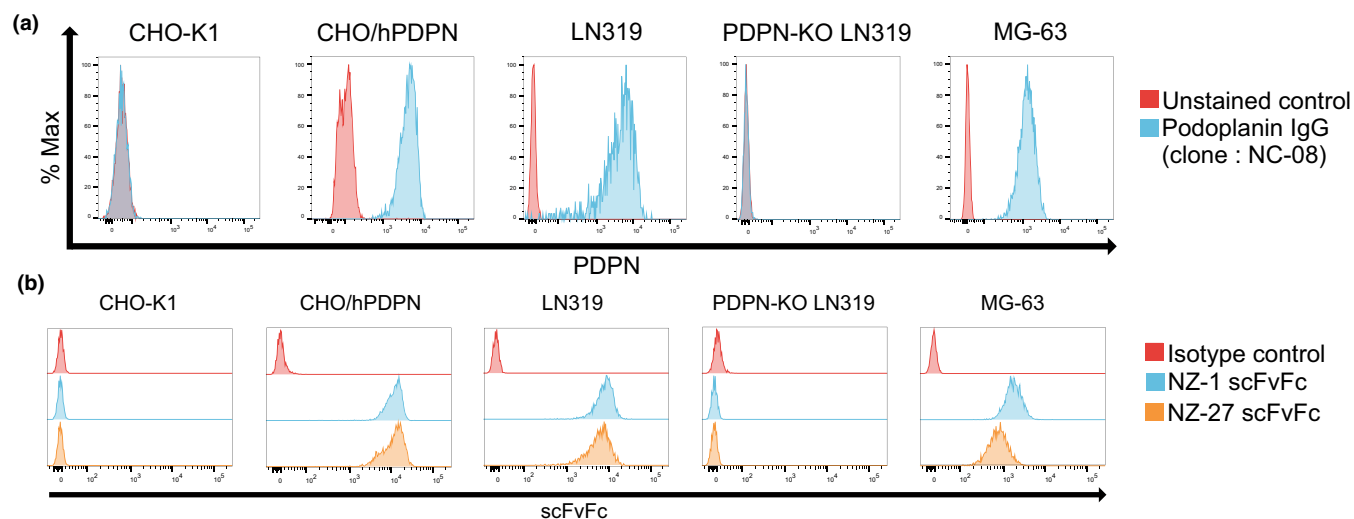### 2.1 | NZ-1 and NZ-27 scFvFc antibodies bind to PDPN-expressing cells

To evaluate whether NZ-1 and NZ-27 scFvFc are effectively attached to PDPN, we first selected PDPN-expressing cells.

LN319, CHO/hPDPN, and MG-63 cells expressed PDPN (Figure 1a), and we confirmed that NZ-1 and NZ-27 scFvFc were able to specifically and similarly bind to PDPN-expressing cells (Figure 1b).
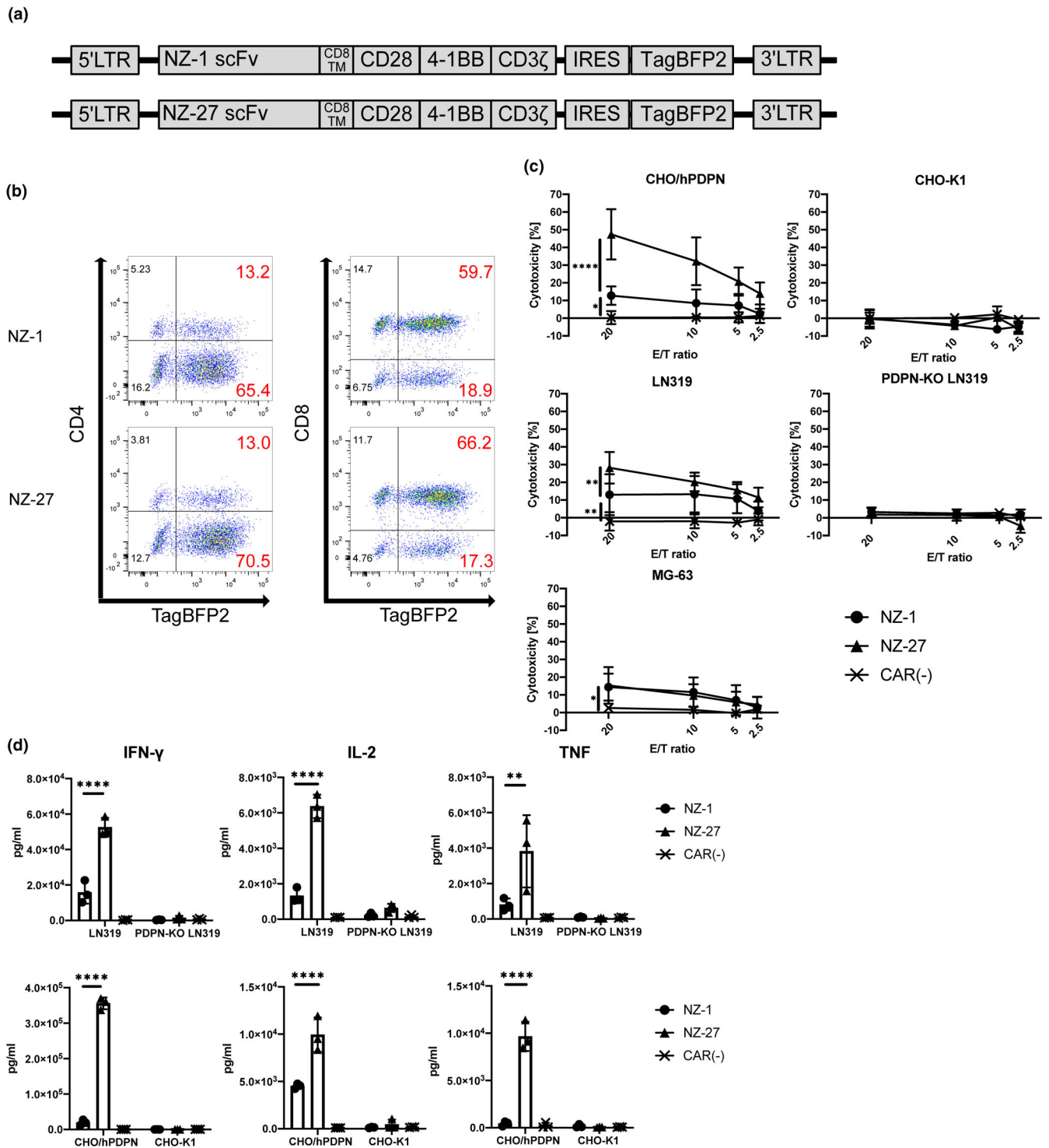
2.2 | NZ-27 CAR-T cells enhanced their cytotoxicity and proinflammatory cytokine production against PDPN-expressing cells compared to NZ-1 CAR-T cells

Third-generation CARs were generated from the scFv part of NZ-1 and NZ-27, and retroviral vectors containing the CARs were transduced into primary T cells (Figure 2a). The transduction efficiency of each CAR gene was evaluated using TagBFP2 fluorescence. Among NZ-1 and NZ-27 CAR-T cells, 13.2 and 13.0% were CD4- and TagBFP2-positive cells and 59.7 and 66.2% were CD8- and TagBFP2-positive cells; totally, 78.6% and 83.5% TagBFP2-positive cells were successfully obtained from NZ-1 and NZ-27 CAR-T cells, respectively (Figure 2b). This result suggests that (1) there was no significant difference in transfection efficiency between NZ-1 and NZ-27 and that (2) NZ-1 and NZ-27 were efficiently transduced into both CD4 and CD8 T cells.

To evaluate whether NZ-1 and NZ-27 CAR-T cells were effective against PDPN-expressing cells, we performed a cytotoxicity assay of CAR-T cells against PDPN-expressing cells. Each CAR-T cell showed E:T ratio-dependent cytotoxicity against LN319, CHO/hPDPN, and MG-63 cells, which express PDPN (Figure 2c). NZ-27 CAR-T cells showed significant cytotoxicity against LN319 and CHO/hPDPN cells compared to that against NZ-1 CAR-T cells, but not against MG-63

FIGURE 1 NZ-1 and NZ-27 scFvFc antibodies bind to PDPN-expressing cells. (a) Flow cytometry plots of PDPN expression of each cell. (b) NZ-1 and NZ-27 scFvFc antibodies binding to PDPN-expressing cells

(a)

| 5'LTR | NZ-1 scFv | CD8 TM | CD28 | 4-1BB | CD3ζ | IRES | TagBFP2 | 3'LTR |

| 5'LTR | NZ-27 scFv | CD8 TM | CD28 | 4-1BB | CD3ζ | IRES | TagBFP2 | 3'LTR |

(b)

(c)

(d)

FIGURE 2 NZ-27 CAR-T cells enhanced their cytotoxicity and cytokine production against PDPN-expressing cells compared to NZ-1 CAR-T cells. (a) Schematic of retroviral constructs encoding NZ-1 and NZ-27 CARs. These were expressed with the IRES-linked TagBFP2 gene. (b) Flow cytometry plots of CD4, CD8, TagBFP2-positive CAR-T cells. (c) In vitro cytotoxicity assay of each CAR-T cell measured using nonradioactive cellular cytotoxicity assay using LN319, PDPN-KO LN319, CHO-K1, CHO/hPDPN, and MG-63 cells ($n = 5$). (d) IFN-γ, IL-2, and TNF expression of each CAR-T cell against PDPN-expressing cells ($n = 3$). Data represent mean ± standard error of the mean of n independent experiments. $*p < .05$, $**p < .01$, and $****p < .001$ using one-way analysis of variance with Tukey's multiple comparison test. CAR, chimeric antigen receptor; IFN-γ, interferon γ; IL-2, interleukin 2; IRES, internal ribosome entry site; PDPN, podoplanin; TNF, tumor necrosis factor
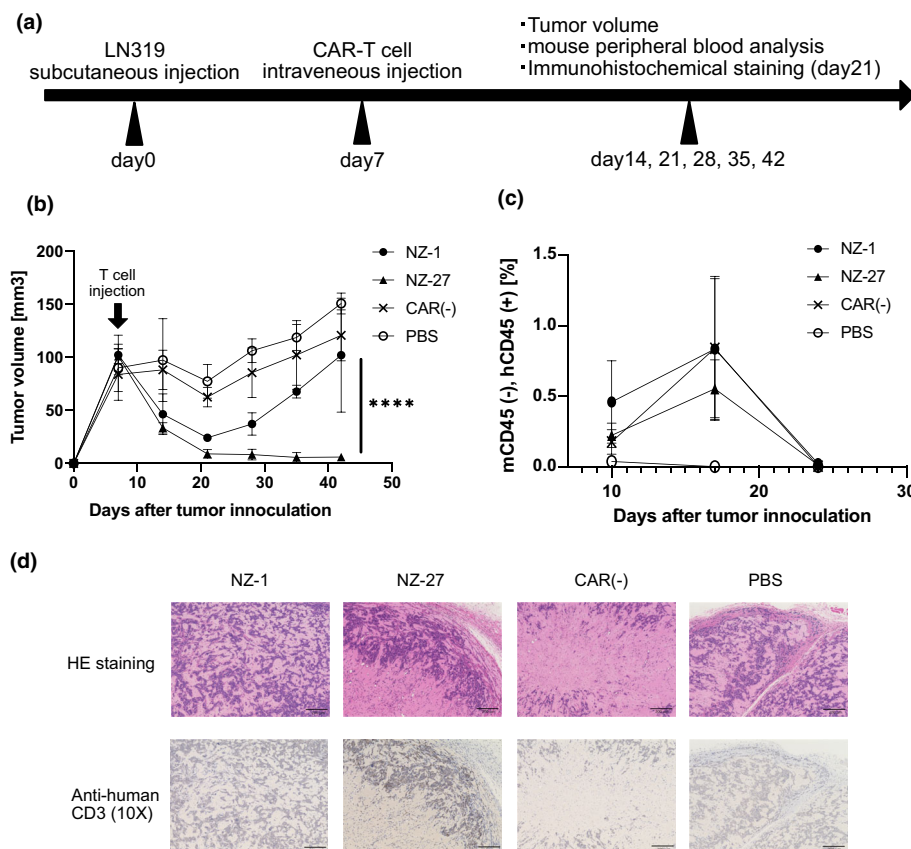
FIGURE 3 NZ-27 CAR-T cells have superior anti-tumor activity against the PDPN xenograft model compared to NZ-1 CAR-T cells. (a) Subcutaneous and intravenous injections of LN319 cells and CAR-T cells, respectively. (b) Monitored for tumor volume. (c) mCD45−, hCD45+ cells in mouse peripheral blood (three mice). (d) Anti-human CD3 antibodies were used for immunohistochemical staining of LN319 cells derived from subcutaneous carcinoma in mice treated using different CAR-T cells. The dotted line indicates human CD3+ cells. Data represent mean ± standard error of the mean of n independent experiments. ****$p < .001$ using one-way analysis of variance with Tukey's multiple comparison test. CAR, chimeric antigen receptor

cells (Figure 2c). NZ-27 scFvFc showed lower affinity to MG-63 cells compared to NZ-1 scFvFc (Figure 1b), suggesting that this is one of the reasons underlying the low cytotoxicity of NZ-27 CAR-T cells against MG-63 cells. Because T-cell cytotoxicity is known to be influenced by the production of proinflammatory cytokines, we evaluated IFN-γ, IL-2, and TNF activation for 24 h after co-culturing CAR-T cells with PDPN-expressing cells. The results showed significantly better expression of IFN-γ, IL-2, and TNF in the supernatant samples containing NZ-27 CAR-T cells than in those containing NZ-1 CAR-T cells (Figure 2d).

2.3 | NZ-27 CAR-T cells have superior anti-tumor activity against the PDPN xenograft model compared to NZ-1 CAR-T cells

To evaluate the anti-tumor activity of different CAR-T cells against PDPN-expressing cells, LN319 cells were subcutaneously injected into NOG mice. Seven days after subcutaneous tumor inoculation, other CAR-T-cells were injected intravenously. Tumor volume and hCD45+ T cell proportion in mouse peripheral blood and T-cell

infiltration into the tumor were evaluated (Figure 3a). As indicated in Figure 3b, tumor progression was suppressed for 14 days in all CAR-T cell-treated groups. The volume recurrently increased in the NZ-1 CAR-T cell-treated group, whereas NZ-27 CAR-T cell-treated groups did not show recurrent tumor progression until day 42.

Since the long-term persistence of T-cells in peripheral blood and the number of infiltrated T-cells in tumor correlate with therapeutic efficacy against cancer (Chen & Mellman, 2013; Park et al., 2016), hCD45+ cell populations in mouse peripheral blood from each T-cell-treated group were periodically evaluated; at 14 days after T-cell injection, tumors were immunohistochemically stained with anti-human CD3 antibodies. hCD45+ cell populations were maintained for 17 days after T-cell injection; however, no significant difference was observed in hCD45+ cell populations in each CAR-T cell-treated group (Figure 3c). Next, we observed the existence of each CAR-T cell that infiltrated the tumor. The group treated with NZ-27 CAR-T cells had more human CD3-positive infiltrated cells than that treated with NZ-1 CAR-T cells (Figure 3d).

These results suggest that NZ-27 CAR-T cells improved their proliferation against PDPN-expressing solid tumors compared to NZ-1 CAR-T cells.

2.4 | Expression of NZ-1 CAR on the cell surface was weakened, making T-cell activation difficult compared to other CARs

We showed that NZ-1 and NZ-27 scFvFc have similar specific affinity against PDPN. However, compared with NZ-1 CAR-T cells, NZ-27 CAR-T cells showed better effector function and anti-tumor efficacy against PDPN-expressing cells. This result was thought to be due to the low expression of NZ-1 CAR on the cell surface and the insufficient total amount of T-cell activation signaling. The Myc tag sequence was inserted downstream of the signal sequence of each CAR to determine the expression level of each CAR on the cell surface, as shown in Figure 4a. Each CAR was expressed in Jurkat NFAT-luc
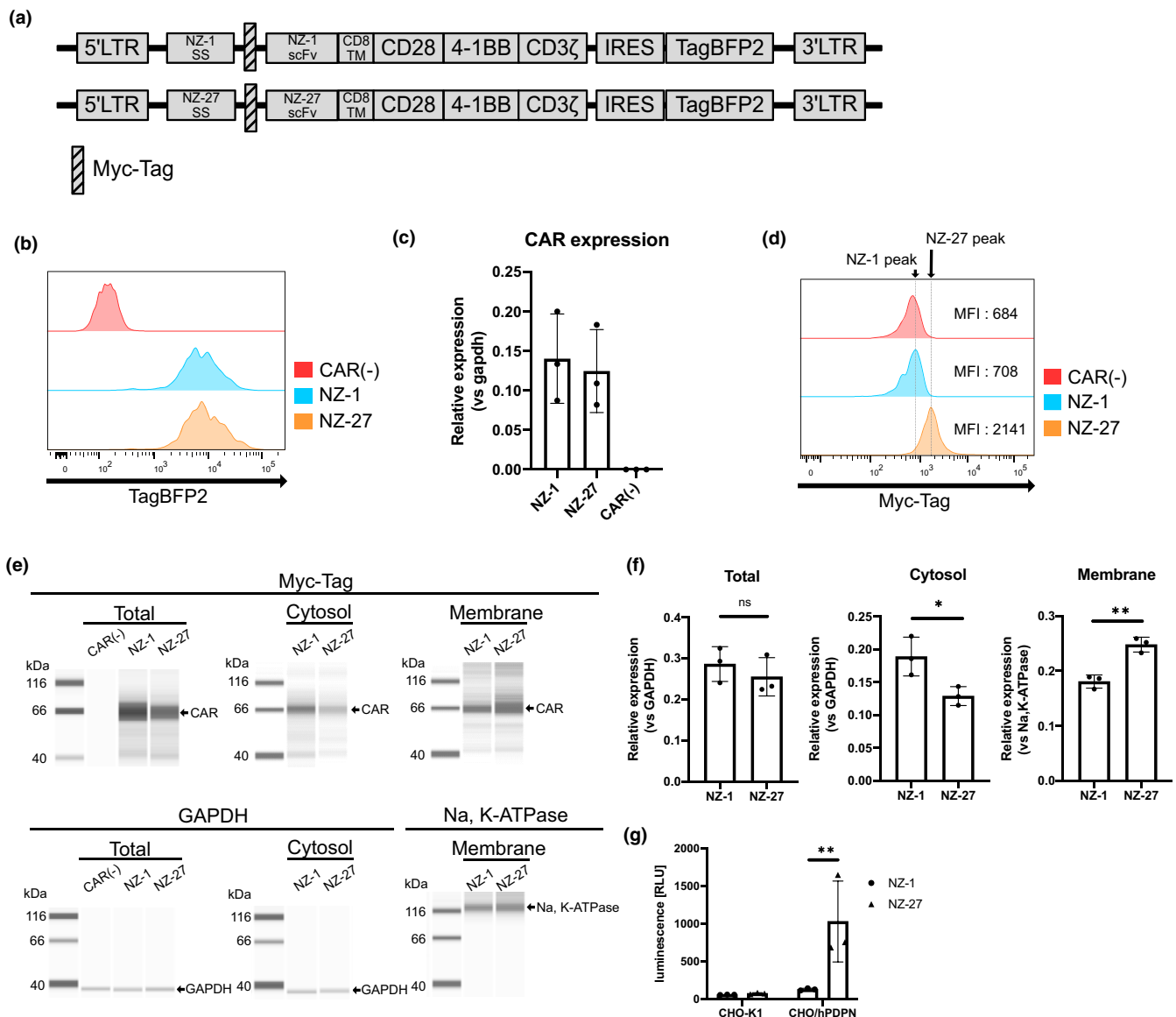
FIGURE 4 Expression of NZ-1 CAR on the cell surface is weakened, making it difficult for T-cell activation compared to other CARs. (a) Schematic of retroviral constructs encoding Myc-Tag-inserted NZ-1 and NZ-27 CARs. These CARs were expressed with the IRES-linked TagBFP2 gene. (b) Flow cytometry plots of each Jurkat NFAT-luc cells with TagBFP2 expression. (c) Each CAR transcription activity was evaluated using qPCR ($n = 3$). (d) Flow cytometry plots of each Jurkat NFAT-luc cells with Myc-Tag expression. Dotted lines indicate the peaks of NZ-1 and NZ-27 CAR-expressing Jurkat NFAT-luc cells. (e) Western blotting assay of each Jurkat NFAT-luc cells with Myc-Tag expression. The results showed expression of Myc-Tag, GAPDH, and Na, K-ATPase. (f) Statistical analysis of results generated by Western blotting ($n = 3$). (g) Luciferase luminescence derived from each CAR stimulation ($n = 3$). Data represent mean ± standard error of the mean of n independent experiments. **$p < .01$, *$p < .05$, and ns using one-way analysis of variance with Tukey's multiple comparison test or Student t-test

cells, a cell line derived from human acute T-cell leukemia cells genetically engineered to express luciferase under NFAT response element upon TCR signal-mediated activation (Clipstone & Crabtree, 1992; Lyakh et al., 1997). As shown in Figure 4a, retroviral vectors were used for gene transfer into Jurkat NFAT-luc cells. The transduction efficiency of each retroviral vector was evaluated by TagBFP2 and mRNA expression at the same level (Figure 4b,c). However, the same CAR mRNA and TagBFP2 protein expression levels were confirmed. Myc-Tag expression, which reflects cell surface CAR expression, was weakened in NZ-1 CAR-expressing Jurkat NFAT-luc cells compared with NZ-27 CAR-T cells (Figure 4d). We further observed NZ-1 and NZ-27 CAR total protein expression levels using the Myc tag. There was no significant difference in the total protein expression levels of NZ-1 and NZ-27 CARs, which was the same result as that obtained with mRNA expression (Figure 4c, e,f). Next, we observed the localization of each CAR and found that NZ-1 CARs and NZ-27 CARs were significantly more abundant in the cytoplasm and plasma membrane, respectively (Figure 4e,f).

Finally, to estimate the strength of TCR signals induced by CAR activation, we co-cultured Jurkat NFAT-luc cells expressing each CAR with CHO/hPDPN cells and quantified luciferase luminescence. Luciferase luminescence was elevated in the co-culture with CHO/hPDPN cells (Figure 4g). Moreover, the luciferase luminescence of NZ-27 CAR-expressing Jurkat NFAT-luc cells was higher than that of NZ-1 CAR-expressing Jurkat NFAT-luc cells (Figure 4g).

These results suggest that one of the reasons for the enhanced anti-tumor effect of NZ-27 CAR-T cells is enhanced T-cell activation associated with higher cell surface expression of NZ-27 CAR compared with that of NZ-1 CAR.

3 | DISCUSSION

In this report, we showed that the different expression levels of NZ-1 and NZ-27 CAR on the cell surface affect the anti-tumor efficacy of CAR-T cells. The effector function of the CAR-T cell depends on the efficiency of insertion and expression of the CAR gene; however, there were no significant differences in the mRNA expression level of NZ-1 and NZ-27 CAR and the total protein expression level of the Myc-Tag inserted into the CAR sequence. These results suggest that the enhanced effector function of NZ-27 CAR-T cells was not due to differences in CAR gene insertion and expression levels. Furthermore, NZ-27 CAR expression on the plasma membrane was higher than that of NZ-1

CAR, suggesting the enhanced effector function of NZ-27 CAR-T cells.

PDPN has four platelet aggregation-stimulating (PLAG) domains in the extracellular domain that bind to C-type lectin-like receptor-2 (CLEC-2). CLEC-2 binds to the PLAG3 domain of PDPN and has been reported to promote cancer cell metastasis (Waseda & Kaneko, 2020). Therefore, the NZ-27 CARs generated in our study will have better anti-tumor activity against PDPN-expressing cells and may preferentially have the potential to suppress cancer metastasis because the NZ-27 epitope is located in the PLAG2-3 domain (Ogasawara et al., 2008).

The scFv that constitutes the CAR contains complementarity-determining regions (CDRs) and framework (FR) regions, which are responsible for antigen specificity and stability(Fujiwara et al., 2020; Guo et al., 2022). The CDR and FR sequences in scFv differ among species, and FR sequences have been reported to change into human immunoglobulin sequences to accommodate immunogenicity in the creation of humanized CAR (Guo et al., 2022). In this report, we created NZ-27 CAR by optimizing the CDR of the NZ-1 CAR to the human codon sequence and changed the FR sequence to that of trastuzumab, a human IgG1 antibody. This change did not alter the mRNA transcript levels or total protein levels of the NZ-1 and NZ-27 CARs but resulted in a significant difference in the expression levels of the CARs on the plasma membrane. It has also been reported that changing only the CDR does not change the total amount of protein but instead changes the amount and stability of expression on the cell membrane (Fujiwara et al., 2020). After a gene is transcribed, various post-translational modifications occur in intracellular organelles and are thought to determine the function, localization, and stability of the protein; thus, we speculated that the difference in post-translational modifications on each CAR and structural differences in CDR and/or FR due to humanization may have caused the expression difference (Moremen et al., 2012; Rape, 2018; Yang & Qian, 2017). The possibility of post-translation modifications related to efficient protein formation and expression on the cell surface in human cells to create highly effective CAR is an interesting topic of study and should be further explored.

In this report, we performed an in vivo experiment using only the LN319 cell line. Therefore, we cannot exclude the possibility that the improvement of anti-tumor efficacy on using NZ-27 CAR-T cells is applicable to the LN319 cell line. In a further study, we would like to evaluate NZ-27 CAR using other PDPN-expressing cell lines and develop a new CAR for PDPN-expressing tumors.

In summary, herein, we demonstrated the usefulness of NZ-27 CAR for PDPN-expressing cells. We found that

in addition to the strength of the affinity for the antigen, the enhancement of activation signals associated with higher CAR expression on the T cell surface is essential for creating functional CAR. Based on the findings of this study, the clinical application of NZ-27 CARs with improved therapeutic efficacy against PDPN-expressing cancer cells is anticipated.

4 | EXPERIMENTAL PROCEDURES

4.1 | Ethical consideration

This study was conducted in accordance with the tenets of the Declaration of Helsinki and was approved by the Institutional Ethical Board of Kyoto University. The Institutional Animal Research Committee approved animal experiments, and all experiments were performed in accordance with relevant guidelines and regulations. Healthy volunteers (from whom PBMCs were obtained) provided written informed consent.

4.2 | Cell lines and peripheral blood mononuclear cells

LN319 and CHO-K1 were purchased from Addexbio Technologies (San Diego, CA) and ATCC (Manassas, VA, USA), respectively. PDPN-KO LN319 and CHO/hPDPN cells were initially generated in our previous study (Kato & Kaneko, 2014). The RIKEN BRC provided the human osteosarcoma cell line MG-63 (RCB1890) through the National BioResource Project of the MEXT/ AMED, Japan. LN319 and PDPN-KO LN319 cells were maintained in Dulbecco's modified Eagle medium supplemented with 10% fetal bovine serum (FBS) and 2 mM penicillin–streptomycin-glutamine (PSG) solution (Sigma–Aldrich Corp., St. Louis, MO). CHO-K1 and CHO/hPDPN cells were maintained in RPMI-1640 medium (FUJIFILM Wako Pure Chemical Corporation, Osaka, Japan) supplemented with 10% FBS and 2 mM PSG solution. MG-63 cells were maintained in minimum essential media (MEM) (Thermo Fisher Scientific Inc., Waltham, MA) supplemented with 10% FBS and 2 mM PSG solution. Peripheral blood mononuclear cells (PBMCs) were used to prepare the primary CAR-T cells. PBMCs were obtained from healthy volunteers. T cells were cultured in α-MEM (Sigma–Aldrich) supplemented with 15% FBS, 2 mM PSG (Thermo Fisher), 50 ng/mL of ascorbic acid 2-phosphatase (Sigma–Aldrich Corp.), and 5 ng/mL of rhIL-7 (Peprotech). When expanding T cells, 5 ng/mL of rhIL-15 (Peprotech) was added to α-MEM. All cell lines were cultured at 37°C with 5% CO_2.

4.3 | Construction of retroviral vector

NZ-1 and NZ-27 scFv antibodies; Myc-Tag-inserted NZ-1 and NZ-27 scFv antibodies; CD8 transmembrane domain; and intracellular domain were amplified using polymerase chain reaction (PCR). KOD One PCR master mixblue (TOYOBO, Osaka, Japan) was used. PCR conditions were as follows: denaturation for 2 min at 94°C, followed by 35 cycles of denaturation at 98°C for 10 s and extension at 68°C for 15 s. Amplified genes were inserted into the pMY retroviral vector (Cell BioLabs, San Diego, CA) using NEBuilder HiFi Assembly (New England BioLabs, Ipswich, MA). The primers are listed in Table S1.

4.4 | Generation of NZ-1 and NZ-27 CAR-T cells

GP293 cells were harvested on a 10-cm dish 2 days before transfection. We transfected the CAR gene-encoded retrovirus vector and VSVG gene-encoded pMD2.G vector (Addgene) 2 days later using DNA transfection reagents. For recombinant retroviral production, we generated HT1080-based packaging cell lines reported previously (Iriguchi et al., 2021). For gene transduction, PBMCs were stimulated with Dynabeads Human T-Activator CD3/CD28 for T-cell expansion and activation (Thermo Fisher). On days 2 and 3, activated T cells were loaded onto 50 μg/mL of retronectin (Takara-bio, Kusatsu, Japan)-coated 96-well plates that were preloaded with retrovirus supernatant. Retronectin-coated 96-well plates were incubated at 4°C overnight. Retrovirus-preloaded retronectin-coated 96-well plates were prepared by centrifuging them for 2 h at 2000 g and 32°C.

4.5 | Flow cytometry analysis

We used an LSR or FACS AriaII flow cytometer (BD Biosciences, Franklin Lakes, NJ). These data were analyzed using the FlowJo software (Tree Star, Ashland, OR). The antibodies used for staining are listed in Table S2. NZ-1 and NZ-27 scFvFc antibodies were developed as described previously (Chandramohan et al., 2013; Kaneko et al., 2020).

4.6 | Cytokine production

The BD Cytometric Bead Array Flex Set System (BD Biosciences) was used to measure human interleukin 2 (IL-2), interferon-γ (IFN-γ), and tumor necrosis factor (TNF) levels. Cell culture supernatants were collected

after 24 h and centrifuged and frozen until use. Approximately 1.0×10^6 resting CAR-T cells were maintained in α-MEM supplemented with 15% FBS, 2 mM PSG, 50 ng/mL ascorbic acid 2-phosphatase, and 5 ng/mL rhIL-7, and were cultured in the presence of 1.0×10^6 LN319, PDPN-KO LN319, CHO/hPDPN, or CHO-K1 cells.

4.7 | Cytotoxicity assay

We used a nonradioactive cellular cytotoxicity assay kit (Techno-Suzuta, Nagasaki, Japan) according to the manufacturer's instructions. Effector cells were pre-enriched with CD8+ and TagBFP2+ T cells using the FACS AriaII flow cytometer (BD Biosciences). Target cells (LN319, PDPN-KO LN319, CHO-K1, CHO/hPDPN, and MG-63 cells) were pulsed with BM-HT reagent at 37°C for 15 min, washed three times, and seeded into 96-well plates at a density of 5×10^3 cells/well. Effector cells were loaded into the wells at effector-to-target (E:T) ratios ranging from 20:1 to 2.5:1 and were co-cultured for 3 h. Then, 40 μl of the co-culture supernatant was mixed with 160 μl of Eu solution, and time-resolved fluorescence was measured using a NIVO plate reader (Perkin Elmer, Waltham, MA). These cells were cultured in α-MEM supplemented with 15% FBS and 2 mM PSG at 37°C with 5% CO_2.

4.8 | Quantitative real-time PCR analysis

The T-cell activation bioassay (NFAT, Promega, Madison, WI) was used to evaluate CAR activation. Jurkat NFAT-luc cells expressing CAR total RNA and complementary DNA were obtained using Sepasol-RNAISuper G (Nacalai Tesque, Kyoto, Japan) and the PrimeScript II 1st strand cDNA synthesis kit (Takara-bio) according to manufacturers' instructions. Real-time quantitative PCR was performed using StepOnePlus (Applied Biosystems, Waltham, MA). Designed primers and PowerUp SYBR green master mix (Thermo Fisher) were used for PCR amplification. We used the standard cycling mode according to the manufacturer's protocol. Expression levels of CAR were normalized to those of glyceraldehyde 3-phosphate dehydrogenase in each sample using the ΔΔCT method.

4.9 | Western blotting assay

To obtain the total protein of Jurkat NFAT-luc cells expressing NZ-1 and NZ-27 CAR, we used RIPA Buffer (FUJIFILM Wako Pure Chemical Corporation) according to the manufacturer's protocol. To obtain cytosol and plasma membrane protein of Jurkat NFAT-luc cells

expressing NZ-1 and NZ-27 CAR, we used Mem-PER™ Plus Membrane Protein Extraction Kit (Thermo Fisher) according to the manufacturer's protocol. In RIPA buffer and protein extraction buffer included in Mem-PER™ Plus Membrane Protein Extraction Kit, Halt™ Phosphatase Inhibitor Cocktail (Thermo Fisher) was added, and 5.0×10^6 Jurkat NFAT-luc cells were used on each assay. Wes (protein simple, San Jose, CA) was used for observing protein expression levels. On each assay, EZ Standard Pack 1 (protein simple), Anti-Rabbit Detection Module for Jess/Wes (protein simple), and Anti-Mouse Detection Module for Jess/Wes (protein simple) were used according to the manufacturer's protocol. Used antibodies were listed in Table S2. Compass software for Simple Western (protein simple) was used to evaluate each expression level.

4.10 | Luciferase assay

To obtain CAR-expressing Jurkat NFAT-luc cells, Jurkat NFAT-luc cells were infected with retrovirus as described above. In total, 1.0×10^5 Jurkat NFAT-luc cells expressing CAR and approximately 1.0×10^5 CHO/hPDPN and CHO-K1 cells were co-cultured at 37°C for 3 h. After co-culture, luciferin (Promega) was added to evaluate luciferase luminescence, measured using a NIVO plate reader.

4.11 | In vivo animal models

Six-week-old female NOD.Cg-PrkdcscidIL-2rgtm1Sug/ShiJic (NOG)_MHC-dKO mice were purchased from CIEA. Approximately 5.0×10^6 LN319 cells mixed with BD Matrigel matrix (growth factor reduced) (BD Biosciences) in a 3:5 ratio (v/v) were injected subcutaneously on day 0. In total, 1.0×10^6 NZ-1 and NZ-27 CAR-positive T cells or 1.0×10^6 CAR-negative T cells were injected intravenously on day 7. These CAR-T cells were infected with the retrovirus as described above. For T-cell expansion and activation, they were injected into mice 7 days after stimulation with Dynabeads human T-activator CD3/CD28. Tumor dimensions were measured with calipers, and tumor volumes were calculated using the formula $V = LW^2/2$, where L is the length (longest dimension), and W is the width (shortest dimension).

4.12 | Analysis of tumor-infiltrating iPS-CAR-T cells

NOG_MHC-dKO mice were sacrificed 14 days after T-cell injection. Immunohistochemical staining was performed

at the Center for Anatomical, Pathological, and Forensic Medical Research at Kyoto University. The anti-human CD3 antibody (clone NCL-CD3-PS1; Leica Biosystems) and Mouse to Mouse HRP staining System (ScyTek Lab., UT) were used to stain the samples. Staining images were captured using a fluorescence microscope (BZ-X800; Keyence, Osaka, Japan).

4.13 | Statistical analyses

Data are represented as mean ± standard deviation or mean ± standard error of the mean. All statistical analyses were performed using GraphPad Prism 8 (GraphPad, San Diego, CA) software. p-values were calculated using one-way or two-way analysis of variance (ANOVA) with Tukey's multiple comparison test and Student's t-test. $*p < .05$, $**p < .01$, $***p < .005$, and $****p < .001$ were considered statistically significant.

CONFLICT OF INTEREST
Shin Kaneko is a founder, shareholder, and chief scientific officer at Thyas Co., Ltd. and received research funding from Takeda Pharmaceutical Co. Ltd., Kirin Co., Ltd., Astellas Co., Ltd., Tosoh Co. Ltd., and Thyas Co., Ltd.

ORCID
Akihiro Ishikawa https://orcid.org/0000-0002-7692-3851
Masazumi Waseda https://orcid.org/0000-0001-7179-5945
Mika K. Kaneko https://orcid.org/0000-0002-4158-9208
Yukinari Kato https://orcid.org/0000-0001-5385-8201
Shin Kaneko https://orcid.org/0000-0003-2291-4586

REFERENCES
Breiteneder-Geleff, S., Matsui, K., Soleiman, A., Meraner, P., Poczewski, H., Kalt, R., Schaffner, G., & Kerjaschki, D. (1997). Podoplanin, novel 43-kd membrane protein of glomerular epithelial cells, is down-regulated in puromycin nephrosis. *The American Journal of Pathology*, *151*, 1141–1152.

Chandramohan, V., Bao, X., Kato Kaneko, M., Kato, Y., Keir, S. T., Szafranski, S. E., Kuan, C. T., Pastan, I. H., & Bigner, D. D. (2013). Recombinant anti-podoplanin (NZ-1) immunotoxin for the treatment of malignant brain tumors. *International Journal of Cancer*, *132*, 2339–2348.

Chen, D. S., & Mellman, I. (2013). Oncology meets immunology: The cancer-immunity cycle. *Immunity*, *39*, 1–10.

Chu, A. Y., Litzky, L. A., Pasha, T. L., Acs, G., & Zhang, P. J. (2005). Utility of D2-40, a novel mesothelial marker, in the diagnosis of malignant mesothelioma. *Modern Pathology*, *18*, 105–110.

Clipstone, N. A., & Crabtree, G. R. (1992). Identification of calcineurin as a key signalling enzyme in T lymphocyte activation. *Nature*, *356*, 695–697.

Fujiwara, K., Masutani, M., Tachibana, M., & Okada, N. (2020). Impact of scFv structure in chimeric antigen receptor on receptor expression efficiency and antigen recognition properties. *Biochemical and Biophysical Research Communications*, *527*, 350–357.

Guo, J., He, S., Zhu, Y., Yu, W., Yang, D., & Zhao, X. (2022). Humanized CD30-targeted chimeric antigen receptor T cells exhibit potent preclinical activity against Hodgkin's lymphoma cells. *Frontiers in Cell and Development Biology*, *9*, 1–10.

Iriguchi, S., Yasui, Y., Kawai, Y., Arima, S., Kunitomo, M., Sato, T., Ueda, T., Minagawa, A., Mishima, Y., Yanagawa, N., Baba, Y., Miyake, Y., Nakayama, K., Takiguchi, M., Shinohara, T., Nakatsura, T., Yasukawa, M., Kassai, Y., Hayashi, A., & Kaneko, S. (2021). A clinically applicable and scalable method to regenerate T-cells from iPSCs for off-the-shelf T-cell immunotherapy. *Nature Communications*, *12*, 1–15.

Jayaraman, J., Mellody, M. P., Hou, A. J., Desai, R. P., Fung, A. W., Pham, A. H. T., Chen, Y. Y., & Zhao, W. (2020). CAR-T design: Elements and their synergistic function. *eBioMedicine*, *58*, 102931.

June, C. H., O'Connor, R. S., Kawalekar, O. U., Ghassemi, S., & Milone, M. C. (2018). CAR T cell immunotherapy for human cancer. *Science*, *359*(6382), 1361–1365.

Kahn, H. J., Bailey, D., & Marks, A. (2002). Monoclonal antibody D2-40, a new marker of lymphatic endothelium, reacts with Kaposi's sarcoma and a subset of angiosarcomas. *Modern Pathology*, *15*, 434–440.

Kaneko, M. K., Ohishi, T., Nakamura, T., Inoue, H., Takei, J., Sano, M., Asano, T., Sayama, Y., Hosono, H., Suzuki, H., Kawada, M., & Kato, Y. (2020). Development of core-fucose-deficient humanized and chimeric anti-human podoplanin antibodies. *Monoclonal Antibodies in Immunodiagnosis and Immunotherapy*, *39*, 167–174.

Kato, Y., Fujita, N., Kunita, A., Sato, S., Kaneko, M., Osawa, M., & Tsuruo, T. (2003). Molecular identification of Aggrus/T1α as a platelet aggregation-inducing factor expressed in colorectal tumors. *The Journal of Biological Chemistry*, *278*, 51599–51605.

Kato, Y., & Kaneko, M. K. (2014). A cancer-specific monoclonal antibody recognizes the aberrantly glycosylated podoplanin. *Scientific Reports*, *4*, 1–9.

Kato, Y., Kaneko, M. K., Kuno, A., Uchiyama, N., Amano, K., Chiba, Y., Hasegawa, Y., Hirabayashi, J., Narimatsu, H., Mishima, K., & Osawa, M. (2006). Inhibition of tumor cell-induced platelet aggregation using a novel anti-podoplanin antibody reacting with its platelet-aggregation-stimulating

domain. *Biochemical and Biophysical Research Communications*, *349*, 1301–1307.

Kato, Y., Sasagawa, I., Kaneko, M., Osawa, M., Fujita, N., & Tsuruo, T. (2004). Aggrus: A diagnostic marker that distinguishes seminoma from embryonal carcinoma in testicular germ cell tumors. *Oncogene*, *23*, 8552–8556.

Kreppel, M., Scheer, M., Drebber, U., Ritter, L., & Zöller, J. E. (2010). Impact of podoplanin expression in oral squamous cell carcinoma: Clinical and histopathologic correlations. *Virchows Archiv*, *456*, 473–482.

Lyakh, L., Ghosh, P., & Rice, N. R. (1997). Expression of NFAT-family proteins in normal human T cells. *Molecular and Cellular Biology*, *17*, 2475–2484.

Mishima, K., Kato, Y., Kaneko, M. K., Nishikawa, R., Hirose, T., & Matsutani, M. (2006). Increased expression of podoplanin in malignant astrocytic tumors as a novel molecular marker of malignant progression. *Acta Neuropathologica*, *111*, 483–488.

Moremen, K. W., Tiemeyer, M., & Nairn, A. V. (2012). Vertebrate protein glycosylation: Diversity, synthesis and function. *Nature Reviews. Molecular Cell Biology*, *13*, 448–462.

Mori, J. I., Adachi, K., Sakoda, Y., Sasaki, T., Goto, S., Matsumoto, H., Nagashima, Y., Matsuyama, H., & Tamada, K. (2021). Anti-tumor efficacy of human anti-c-met CAR-T cells against papillary renal cell carcinoma in an orthotopic model. *Cancer Science*, *112*, 1417–1428.

Myers, R. M., Li, Y., Leahy, A. B., Barrett, D. M., Teachey, D. T., Callahan, C., Fasano, C. C., Rheingold, S. R., DiNofia, A., Wray, L., Aplenc, R., Baniewicz, D., Liu, H., Shaw, P. A., Pequignot, E., Getz, K. D., Brogdon, J. L., Fesnak, A. D., Siegel, D. L., … Maude, S. L. (2021). Humanized CD19-targeted chimeric antigen receptor (CAR) T cells in CAR-Naive and CAR-exposed children and young adults with relapsed or refractory acute lymphoblastic leukemia. *Journal of Clinical Oncology*, *39*(27), 3044–3055.

Ogasawara, S., Kaneko, M. K., Price, J. E., & Kato, Y. (2008). Characterization of anti-podoplanin monoclonal antibodies: Critical epitopes for neutralizing the interaction between podoplanin and CLEC-2. *Hybridoma*, *27*, 259–267.

Park, J. H., Geyer, M. B., & Brentjens, R. J. (2016). CD19-targeted CAR T-cell therapeutics for hematologic malignancies: Interpreting clinical outcomes to date. *Blood*, *127*, 3312–3320.

Rape, M. (2018). Post-translational modifications: Ubiquitylation at the crossroads of development and disease. *Nature Reviews. Molecular Cell Biology*, *19*, 59–70.

Scarfò, I., & Maus, M. V. (2017). Current approaches to increase CAR T cell potency in solid tumors: Targeting the tumor microenvironment. *Journal for Immunotherapy of Cancer*, *5*, 28.

Schacht, V., Dadras, S. S., Johnson, L. A., Jackson, D. G., Hong, Y., & Detmar, M. (2005). Up-regulation of the lymphatic marker podoplanin, a mucin-type transmembrane glycoprotein, in human squamous cell carcinomas and germ cell tumors. *The American Journal of Pathology*, *166*, 913–921.

Shiina, S., Ohno, M., Ohka, F., Kuramitsu, S., Yamamichi, A., Kato, A., Motomura, K., Tanahashi, K., Yamamoto, T., Watanabe, R., Ito, I., Senga, T., Hamaguchi, M., Wakabayashi, T., Kaneko, M. K., Kato, Y., Chandramohan, V., Bigner, D. D., & Natsume, A. (2016). CAR T cells targeting podoplanin reduce orthotopic glioblastomas in mouse brains. *Cancer Immunology Research*, *2*, 259–269.

Waseda, M., & Kaneko, S. (2020). Podoplanin as an attractive target of CAR T cell therapy. *Cell*, *9*(9), 1971.

Yang, X., & Qian, K. (2017). Protein O-GlcNAcylation: Emerging mechanisms and functions. *Nature Reviews. Molecular Cell Biology*, *18*, 452–465.

SUPPORTING INFORMATION

Additional supporting information can be found online in the Supporting Information section at the end of this article.

How to cite this article: Ishikawa, A., Waseda, M., Ishii, T., Kaneko, M. K., Kato, Y., & Kaneko, S. (2022). Improved anti-solid tumor response by humanized anti-podoplanin chimeric antigen receptor transduced human cytotoxic T cells in an animal model. *Genes to Cells*, *27*(9), 549–558. https://doi.org/10.1111/gtc.12972